JOURNAL OF SPACECRAFT AND ROCKETS
Vol. 42, No. 6, November–December 2005

Trajectory Analysis and Staging Trades for Smaller Mars Ascent Vehicles

John C. Whitehead*
Lawrence Livermore National Laboratory, Livermore, California 94551

Mars ascent trajectories are calculated for small-scale vehicles that would improve the affordability of Mars sample return. Vehicle size, thrust levels, staging, and the importance of atmospheric drag are all taken into consideration. The high acceleration of conventional solid rockets requires a steep trajectory for drag avoidance, followed by a relatively large circularization burn, appropriate for a second stage. Lower thrust reduces total Δv because reduced drag permits less steep trajectories that require small circularization burns. The results suggest the development of miniature liquid-propelled vehicles or advanced solid rockets having reduced thrust and multiple-burn capability.

Introduction

A NASA-funded study by the National Research Council in 2003 placed a high priority on Mars sample return (MSR) missions.[1] More recently, the case for MSR has been strengthened by the exciting geology results from Jet Propulsion Laboratory's Mars Exploration Rovers.[2] However, a MSR mission has not been planned in detail, because of the high cost and incomplete technology readiness. One missing ingredient is a Mars ascent vehicle (MAV).

Mission costs are on the order of $1M/kg for payloads landed on Mars, typically just hundreds of kilograms. A MAV as small as 100 kg could save hundreds of millions of dollars per MSR mission attempt, compared to MAV designs that exceed 300 kg. A MAV must deliver a 4-km/s velocity change in minutes, with guidance and control to reach orbit. No rocket system ever built near the size of interest has had such high performance.

Various potential MAV designs have been studied, with consideration of both liquid and solid propellants.[3–9] The author has suggested miniaturization of pump-fed liquid rocket technology to achieve high propellant fractions.[10–12] Studies of individual MAV designs have included trajectory analysis.[13] The present paper is intended to address the Mars ascent trajectory problem more generally.

A commonly used type of rocket trade study calculates the required vehicle mass needed to deliver a specified payload, using myriad engineering assumptions for each of multiple alternatives. Then, the smallest vehicle design is recommended from among several choices. If the underlying technologies are not yet available, the assumptions must be drawn from incomplete information. Therefore, the conventional method can yield results of limited applicability, while offering limited fundamental insight. The approach used herein is intended to avoid the need for MAV design details. The general problem is to quantify and understand the significance of trajectory considerations for propulsion choices and staging options, as Mars ascent vehicles are made smaller than is presently possible.

Smaller vehicles have more area per unit mass, and so drag is significant even in Mars' thin atmosphere. Conventional solid rockets reach high speeds sooner than liquids, so that drag affects trajectory selection depending on propulsion choices. This paper presents the results of trajectory calculations for a range of Mars launch masses down to 50 kg, focusing on a 100-kg MAV. Additional analysis is done to address specific questions related to staging, vehicle shape, and thrust preferences. Conclusions drawn from this work can be used to guide technology development that might permit Mars ascent on a smaller scale.

Received 5 May 2004; presented as Paper 2004-4069 at the AIAA/ASME/SAE/ASEE 40th Joint Propulsion Conference, Fort Lauderdale, FL, 11–14 July 2004; revision received 4 January 2005; accepted for publication 6 January 2005.

*Senior Scientist, P.O. Box 808, Mail Stop L-413. Senior Member AIAA.

Fundamentals of Reaching Orbit

Figure 1 depicts two paths to orbit, labeled A and B, where R is the radius of the orbit and r is the radius of the planet. Each path consists of two propulsive maneuvers, numbered 1 and 2. Path A has a horizontal launch directly into an elliptical orbit, which is circularized. After a vertical launch, the path B vehicle coasts to a stop at the desired altitude, then it executes a very large circularization burn. Both paths are extreme cases that are never used, but they offer insight because all real trajectories are somewhere in between.

If there is no atmosphere and no hills to hit, the least total Δv to orbit is obtained by following path A using infinite thrust. In reality, finite acceleration requires some initial vertical velocity to avoid the terrain. Vacuum conditions can favor solids over liquids because solids can more closely follow path A because of their higher acceleration. However, avoiding excess drag in an atmosphere requires a substantial initial vertical component, to gain altitude early. Very dense atmospheres tend to favor path B. Drag avoidance can also favor liquids because more altitude can be gained at lower speeds than with solids. Detailed calculations are needed to assess a particular situation.

The path followed affects Δv greatly. It is enlightening to quantify the inefficiency of path B under ideal conditions, that is, the Δv for path B relative to path A. Equations for physical laws lead to

$$\frac{\Delta v_B}{\Delta v_A} = \frac{\Delta v_{B1} + \Delta v_{B2}}{\Delta v_{A1} + \Delta v_{A2}} = \frac{\sqrt{2 - 2r/R} + \sqrt{r/R}}{\sqrt{2/(1 + r/R)} + \sqrt{r/R} - \sqrt{2/[(1 + R/r)R/r]}} \tag{1}$$

The assumptions are a nonrotating planet, inverse-square gravity, no atmosphere, infinite thrust (zero-duration impulsive maneuvers), and circular orbits. Equation (1) is independent of the gravitational constant and planet mass because the square root of their product was initially present in all terms on the right-hand side. Factoring out these physical quantities leaves each individual velocity component normalized to orbital velocity at zero altitude.

In the numerator, Δv_{B1} is from conservation of energy, while equating centripetal acceleration to gravity yields Δv_{B2}. Conservation of angular momentum was additionally used to obtain the first and last terms in the denominator. The last two radicals in the denominator represent Δv_{A2} as the difference between the normalized

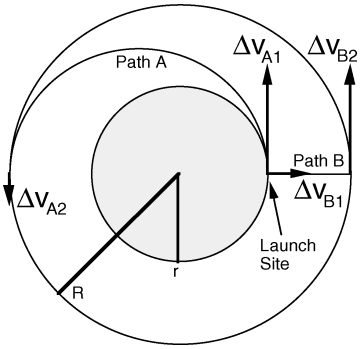

Fig. 1 Two extreme paths to orbit.

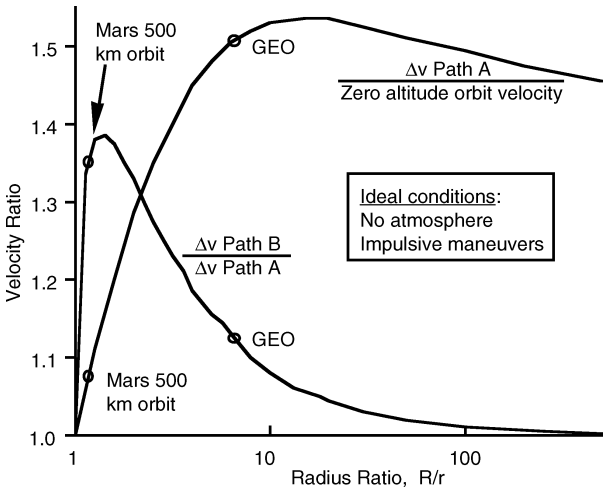

Fig. 2 Semilogarithmic plot of Eq. (1).

circular velocity at R and the normalized elliptical arrival velocity at R. Equation (1) was manipulated to require only the ratio of radii.

Equation (1) and its denominator are plotted in Fig. 2. At both extremes, the $\Delta v_B/\Delta v_A$ curve has unity values. The reason is that the two paths are the same if $R/r = 1$ ($\Delta v_{B2} = \Delta v_{A1}$ and the others are zero) or if R/r is infinity ($\Delta v_{A1} = \Delta v_{B1} =$ escape velocity). What happens in between applies to real altitudes. An orbit 500 km above Mars is sufficiently long lived to ensure sample retrieval. This desired altitude is close to the worst case for choosing path B over path A. The second curve shows that the ideal Δv_A at 500 km is about 7% higher than the velocity of the lowest orbit. Also illustrated is the fact that the ideal Δv to high orbits [e.g., geosynchronous Earth orbit (GEO)] exceeds escape velocity (square root of 2).

In addition to the inefficiency of not following the ideal path A, real launch vehicles must deliver extra Δv to overcome aerodynamic drag and gravity losses resulting from finite thrust. It is necessary to compromise between high drag losses (too close to path A) and trajectory inefficiency (too close to path B).

One last fundamental fact is true for the idealized cases in Fig. 1, and it is also true for all real ascent trajectories. An orbit is a path that repeats itself, so that the vehicle will return to the point where the last maneuver ends. The important implication for propulsion design is that the last burn must end at orbital altitude.

If conventional solid motors are used, at least two stages are therefore required. If thrust can be gradually reduced from the magnitude required for launch, then it is possible to use continuous (or nearly so) thrusting all of the way to orbit. Although multistage vehicles inherently reduce thrust, a single-stage MAV should not be ruled out. Aside from throttling back during one continuous burn, a microgravity restart capability would permit a separate circularization burn for either a single-stage vehicle or an upper stage.

Parameters and Model Assumptions

The historical literature includes trajectory analysis for Mars ascent, even before the density of Mars' atmosphere was known.[14]

Table 1 Fixed parameters for Mars calculations

Parameter	Value
Mars gravitational parameter, GM	4.28 (10^{13}) N-m^2/kg
Mars mean radius (assumed spherical)	3380 km
Atmospheric density at surface	0.017 kg/m^3
Atmosphere scale height (1/e decay)	8.3 km
Speed of sound	250 m/s

Table 2 Velocities from physical constants

Velocity for Mars vacuum flight	Value, m/s
Orbital velocity at zero altitude	3559
Orbital velocity at 500 km altitude	3322
Path A Δv to 500 km orbit	3796
Δv_{A1}	3679
Δv_{A2}	116
Path B Δv to 500-km orbit	5128
Δv_{B1}	1807
Δv_{B2}	3322

Table 3 Vehicle and propulsion initial assumptions

Quantity	Value
Frontal area (reference for drag)	0.2 m^2
Low-speed drag coefficient	0.2
Total mass at launch	100 kg
Solid specific impulse	280 s
Thrust of conventional solid motor	10,000 N
Liquid specific impulse	310 s
Liquid thrust	1000 N

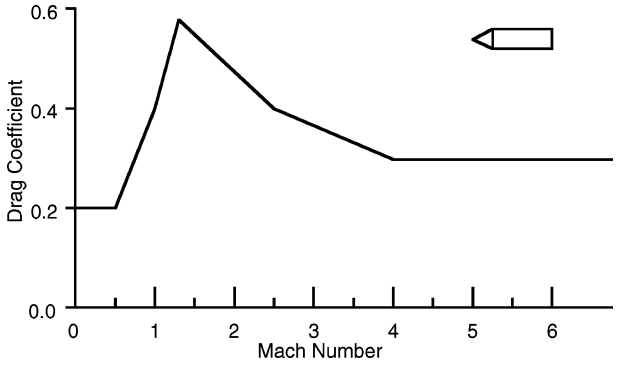

Fig. 3 Drag coefficient variation.

The Viking missions to Mars provided the first direct atmospheric measurements in 1976.[15] A simple exponential decay curve of density with altitude was fit to the data and used herein. Table 1 shows the density assumption along with other fixed constants used to represent Mars.

The first two items in Table 1 yielded the velocities in Table 2, using the analytical equations. Finite thrust, propellant consumption, and aerodynamic drag were subsequently included in trajectory simulations, using numerical integration of velocity and position over time. The ascent model required all of the items in Table 1.

Table 3 provides baseline simulation parameters that represent vehicle design items for a 100-kg MAV. The high thrust listed for the conventional solid rocket option is typical of motors having propellant loads in the range 60–80 kg. A piecewise linear function, Fig. 3, was used to set the drag coefficient in the ascent simulations. This function approximates an idealized curve corresponding to the projectile shape shown as an inset.

A 100-kg MAV having the 4:1 aspect ratio shown would have a diameter of about 0.4 m (16 in.). Actual drag is increased by nonidealities in vehicle shape and surface texture, as well as by off-axis

flow. Therefore, the frontal area used in the simulations is based on a larger 0.5 m diam. Although solid propellant is denser than liquid, much of the vehicle volume is not propellant. In the absence of detailed designs, it was assumed that the propellant choice would not affect the MAV volume or shape.

Trajectory Simulation Results

Numerical accuracy of the model was verified by obtaining closed circles from initial conditions calculated independently for circular orbits, with no atmosphere. For the ascent simulations, initial velocities were zero for launch, that is, the nonrotating planet assumption. The propellant quantity for the initial ascent burn was treated as a variable. The launch angle was then varied to obtain an apoapsis at the desired orbital altitude without active steering.

Results from simulation runs, using Table 3 values, are listed in Table 4. Each case represents the least total Δv to reach a 500-km circular orbit above Mars. Note that the solid rocket ascent in vacuum is almost identical to the ideal path A to orbit because of high thrust. The liquid ascent in vacuum has a significant gravity loss because thrust is only about 2.7 times the Mars launch weight (100 kg $\times$ 3.75 m/s^2 gravity).

The last two rows of Table 4 indicate that Mars' atmosphere, although extremely thin, is still a significant obstacle to tiny ascent vehicles. Relative to path A, there is a 10–15% Δv increase. Unlike in vacuum, the best solid Δv is higher than the best liquid Δv for a 100-kg MAV.

Although the conventional solid rocket option has a very significant circularization maneuver, Mars ascent with drag and gravity losses is still much better than path B. Figure 4 shows the different trajectories. The apogee longitudes and times across the top of the graph are naturally ordered oppositely to the magnitudes of the circularization burns. The thrust termination points are indicated as small circles on the magnified inset graph. The conventional solid rocket reaches full speed very early, and so it climbs steeply through the atmosphere to avoid excessive drag.

The vertical thrust component at the moment of launch must be at least high enough to lift the vehicle's weight. This rule limits the range of launch angles for both vacuum cases. Figure 4 shows that the liquid trajectory in vacuum starts close to vertical but is essentially horizontal at burnout. Thereafter, this particular ascent

Table 4 Simulation results for baseline MAV designs

Ascent option	Initial Δv, m/s	Circularization Δv, m/s	Total Δv, m/s	$\Delta v/\Delta v_A$
Solid in vacuum	3681	118	3799	1.001
Liquid in vacuum	3856	111	3967	1.045
Solid in atmosphere	2803	1567	4371	1.151
Liquid in atmosphere	3900	257	4157	1.095

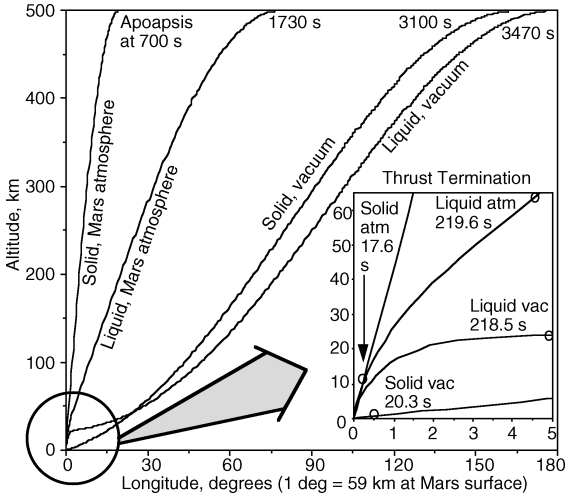

Fig. 4 Baseline MAV trajectory profiles.

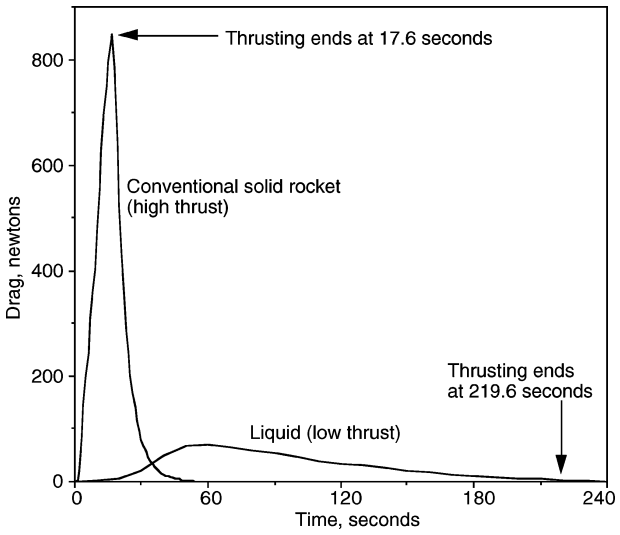

Fig. 5 Mars atmospheric drag.

trajectory amounts to a 24 $\times$ 500 km elliptical orbit. The 24-km periapsis altitude is consistent with a circularization Δv (Table 4) less than for path A (Table 2).

Drag during the baseline atmospheric trajectories is plotted in Fig. 5. The solid-propelled MAV experiences increasing drag, up until stage 1 thrust termination. The curve then plummets as the vehicle slows and exits the atmosphere. The liquid-propelled MAV spends more time in the atmosphere, but at lower speeds. Its drag curve decays to a negligible level by the time of thrust termination. The drag peaks for these very different trajectories are a similar fraction of each one's own thrust level, 8.5 and 7% for solid and liquid, respectively.

Extra propellant consumption is related to the integral of drag, not the magnitude. The areas under the solid and liquid curves are 11,850 and 6580 N-s, respectively. Dividing by specific impulses indicates that 4.3 kg of solid propellant, or 2.2 kg of liquid propellants, would be consumed to overcome drag.

A more complete comparison can be cast in terms of propellant quantities, by simply using the rocket equation with the numbers listed in Table 4. Neglecting staging,

$$\Delta v = I_{SP} g_0 \ell_n (m_i / m_f) \tag{2}$$

where I_{SP} is specific impulse referenced to Earth weight as in Table 3, g_0 is Earth's gravitational acceleration, m_i is the initial total vehicle mass (100 kg here), and m_f is the final mass after expending propellant. From Eq. (2), propellant masses of 79.7 kg (solid) and 74.5 kg (liquid) were calculated. Much of the difference is caused by specific impulse, for example, reaching the liquid Δv at the I_{SP} of the solid rocket requires 78.0 kg of propellant. The differences in drag, gravity losses, and trajectory efficiency account for the rest.

Considering the four paths to orbit, and the drag calculations, it could be said that the lower thrust level offers the better compromise between gravity losses and drag losses. Nothing so far is conclusive for propulsion choices because there are other factors to take into account, notably staging. For example, a solid-propelled MAV would have at least two stages if conventional single-burn motors are used.

MAV Design and Propulsion Questions

Propulsion choices affect trajectory selection, which in turn drives propulsion requirements. Therefore, further analysis can help to answer practical questions, such as those listed here.

1) How many stages, and how should Δv be split among them?

2) Tall narrow MAV with tilt-up launcher, or short wide MAV?

3) What thrust magnitude minimizes delivered Δv?

4) Does it help to reduce solid thrust for trajectory efficiency, considering that slower-burning mixtures might reduce I_{SP}?

5) Does less liquid thrust reduce engine mass by a greater amount than the extra propellant required by a higher Δv trajectory?

6) What is the trade for a liquid restart to circularize, compared to a low-thrust sustainer burn that keeps the tanks settled?

7) Do the results apply to a smaller MAV or a larger MAV?

8) Can a 100-kg solid-propelled MAV be built?

9) Can a 100-kg liquid-propelled MAV be built?

The baseline simulation results have already shed light on some of these questions. The rest of this paper will address the issues in more detail, separately for solid and liquid propulsion. Additional trajectory calculations will be presented for special cases that depart from the baseline vehicle design parameters.

Solid Staging Analysis

From Table 4, a MAV based on conventional solid motors would have two stages, with almost $\frac{2}{3}$ of the Δv on stage 1, to obtain the least total Δv to orbit. However, a different Δv split might improve the net combination of trajectory performance and vehicle performance, even though total Δv would be greater. Figure 6 shows how total Δv increases as the share for each stage departs from the design point of Table 4. As described before, the total Δv was determined at each selected stage 1 propellant load (x axis). The staging question can now be formulated as follows. Given attainable propellant mass fractions for solid rocket stages, which point in Fig. 6 maximizes the payload?

If the stages are 100% propellant with mass-less hardware, then the Δv share for each stage does not affect the MAV design, so that the least total Δv trajectory remains the best. To understand the more practical cases, a range of staging options was calculated from the rocket equation using Fig. 6 data. Figure 7 is the resulting contour plot of payload and the Fig. 6 abscissa, with stage propellant fractions chosen as the independent variables.

Much can be appreciated from a careful study of Fig. 7. Any point along the 64-kg contour represents use of the least total Δv trajectory (note 64-kg point in Fig. 6). This contour intersects the upper-right corner of the graph, at the point of maximum payload and mass-less stage hardware, for the reason already noted. However, the maximum payload point attainable in reality might not be along the 64-kg contour, depending on stage propellant fractions that can actually be achieved.

As would be expected, a trend across Fig. 7 is that better stage 1 technology ($+x$ direction) increases the desired stage 1 propellant load. Conversely, improving stage 2 technology ($+y$ direction) reduces the stage 1 propellant load. The diagonal dashed line represents equal propellant fractions for the two stages. Moving to heavier hardware along the dashed line reduces the size of stage 1. In such cases, the desired design point shifts to the left in Fig. 6 because a more equal Δv split is preferred. In essence, the overall design can suffer from stage 1 inert mass, if the first stage carries more than its best share of the total Δv. At the lower-left corner of Fig. 7, the dashed line approaches the 56-kg contour, near the point of equally shared Δv per Fig. 6.

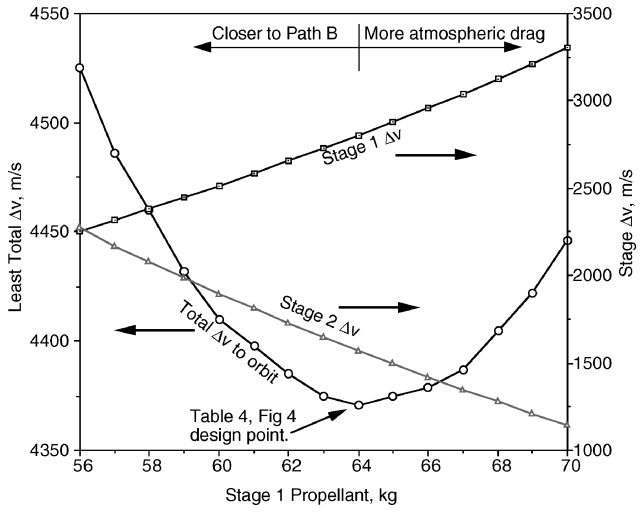

Fig. 6 Velocity variation with solid stage share.

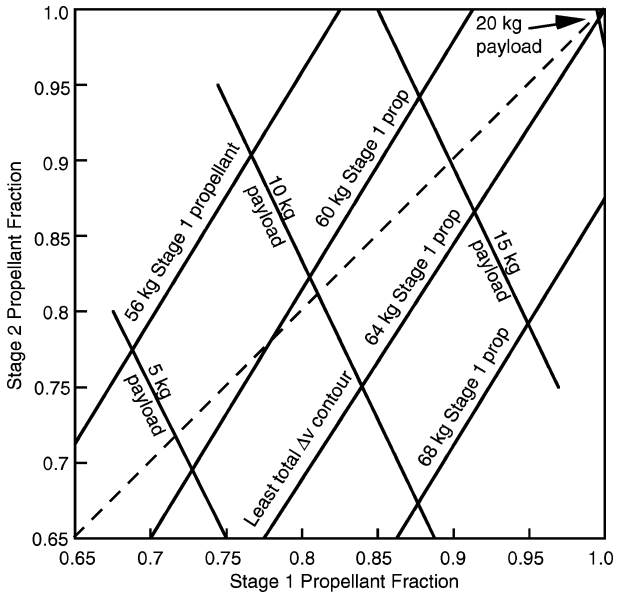

Fig. 7 Effect of solid stage propellant fractions.

Figure 7 provides a useful overview of the two-stage solid-propelled MAV design trade, in which the physical realities of conventional motors and Mars ascent trajectories are implicit. The remaining unknown is, what propellant fractions are possible for complete solid rocket stages (not just motors) that mass roughly 70–80 kg total for stage 1 and about 15 kg for stage 2. In general, larger stages can have better propellant fractions than smaller ones because of the difficulties of miniaturization. An example of such a point is 84% propellant in stage 1, at 75% for stage 2, which would permit a 10-kg payload per Fig. 7. The initial and burnout masses of stage 2 are 13.8 and 3.45 kg, which indicates the extent of miniaturization needed. This design point is on the 64-kg contour, so that it happens to use the best trajectory.

To consider a different example, it is likely that stage 1 needs more guidance and control hardware for atmospheric flight, and perhaps stage 2 could be little more than a bare solid rocket motor if spin stabilization is used. The region above and to the left of the dashed line would apply to a minimum-mass second-stage approach. However, even if stage 2 could have a very high propellant fraction at its small size (e.g., just 1 kg of hardware for a 10-kg propellant grain), the steep slope of the payload contours in Fig. 7 does not permit a particularly poor propellant fraction for stage 1. The payload contour slope partly reflects the trajectory preference for more Δv on stage 1.

A more general interpretation of the steep payload contours is that the feasibility of a two-stage solid-propelled MAV depends heavily on what propellant fraction can be achieved for stage 1. If it is only 75%, for example, Fig. 7 shows that it would be essentially impossible for a 100-kg MAV to deliver a 10-kg payload. The latter includes not just the Mars geology samples, but also their packaging and everything else needed, other than rocket stages.

The interpretation of Fig. 7 might seem contrary to conventional wisdom for launch vehicles. In particular, payload capacity is known to be more sensitive to upper-stage weight growth than to lower-stage weight growth. This rule of thumb applies to Earth launch because extra weight on a first stage is not in itself a problem. There is no contradiction, for two reasons. First, comparing propellant fractions is not the same thing as considering changes in stage absolute mass. Second, the total launch mass on Mars is limited. In terms of the conventional wisdom, stage 1 of the MAV is in reality an upper stage above many others in the MSR mission stack.

Consider what would happen if the staging point selection could be entirely independent of trajectory considerations. The total Δv curve in Fig. 6 would be a horizontal line at the least Δv. Maximizing

the payload then depends only on vehicle design, that is, stage inert masses. There would be no least total Δv contour in a graph like Fig. 7. There would be no advantage to unequal Δv sharing between stages having equal propellant fractions. Separation of vehicle design from trajectory design does happen for liquid propulsion because the staging point can be chosen independently from the two Δv events.

Liquid Staging Analysis

The liquid Δv split shown in Table 4 is too unequal to efficiently use a separate stage just for circularization (6% of the total Δv). Whether the two-burn ascent is accomplished with two stages or just one, an engine restart is needed to circularize the orbit at 500 km above Mars. Therefore, staging considerations are essentially independent of the trajectory, for liquids. The requirement is simply to deliver the total amount of Δv necessary to follow the chosen trajectory.

A liquid version of Fig. 6 does not exist, and Fig. 8 was generated directly from the rocket equation and the total Δv requirement of 4157 m/s. For each chosen pair of propellant fractions for the two stages (x,y), the size of the first stage (parameterized as propellant mass) was varied to maximize the payload. The resulting mass values were initially labeled on the field, then replaced with two sets of contours to facilitate visual interpretation.

Figure 8 has a very different appearance from Fig. 7 because every point on the liquid graph represents the same Δv. The propellant contours all converge at the mass-less hardware point, for a simple reason. In the absence of rocket hardware realities in the upper-right corner of the graph, the liquid trade has nothing left to bias the Δv split. Comparing the payload contours between the solid and liquid graphs indicates that a 15-kg payload capability, for example, might be easier to obtain using liquid, depending on propulsion hardware realities. A 100-kg liquid MAV might even lift 20 kg, which is not possible for a conventional solid rocket within the same mission mass budget.

The liquid trade shows that two stages should share the Δv equally to maximize payload, but only if they can be built to have the same propellant mass fractions. In particular, the propellant contour angled at 45 deg represents the mass that stage 1 must burn (at $I_{SP} = 310$ s) to obtain half of the Δv. The graph is symmetrical about the diagonal, except for the propellant masses. As was the case for the solid stage trade, a higher propellant fraction for stage 1 tends to increase its mass and Δv share. An actual MAV design point would most likely not be on the diagonal. For example, if stage 1 is 80% liquid and stage 2 is at 70%, Fig. 8 shows that the payload would be about 12 kg.

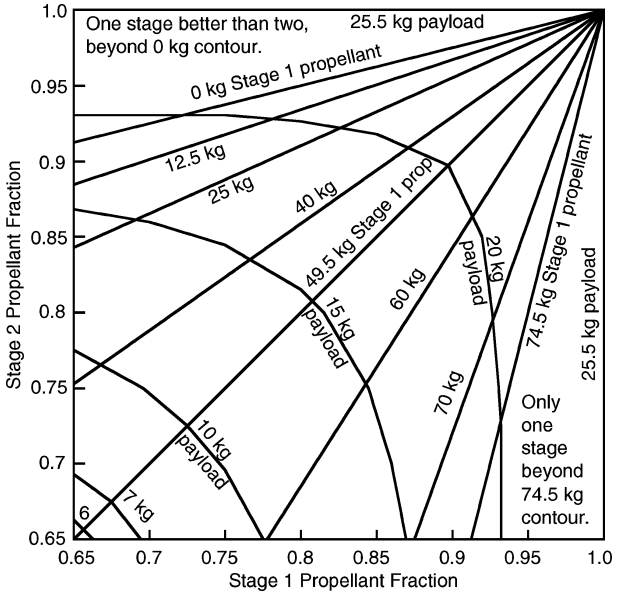

Fig. 8 Effect of liquid stage propellant fractions.

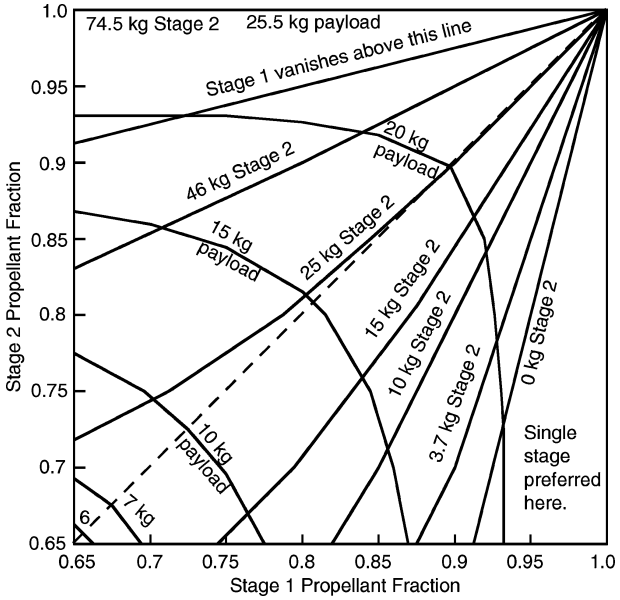

Fig. 9 Stage 2 mass contours on Fig. 8 graph.

There is a triangular region along the right side of Fig. 8, beyond the 74.5-kg propellant contour. The stage 1 propellant load does not rise further within the triangle because 74.5 kg is sufficient to reach orbit. The second stage actually vanishes within that region of the graph, that is, a single-stage MAV delivers the most payload therein. The payload trades directly with stage hardware, so that payload mass contours inside the triangle are exactly vertical. A 25.5-kg payload contour (100–74.5) is along the right border of the graph, where stage 1 inert mass equals zero.

The payload limit contour also extends along the top of the graph. There is another symmetrical triangular single-stage region above the 0-kg stage 1 propellant contour because the math alone does not rule it out. If stage 2 has a very high propellant fraction and that of stage 1 is rather poor, then stage 1 vanishes, and stage 2 stands alone.

Figure 9 was plotted using the same set of calculations to show how small stage 2 must be for a given design point. The 80%, 70% point considered previously has a 15-kg upper stage. Thirty percent of that, or 4.5 kg, would be budgeted for actually building the upper-stage hardware. The latter includes propulsion and control capability.

The practical size of the single-stage region is larger than Fig. 8 indicates because the second stage becomes exceedingly small before the mathematical border is reached. For example, the point at 90% for stage 1 and 70% for stage 2 has a 3.7-kg upper stage per Fig. 9. It would have 2.6 kg of liquids and only a 1.1-kg empty mass. A larger 10-kg upper stage atop a 90% first stage would need to be 80% propellant, which still allows only 2 kg for hardware. There is always the option to sacrifice payload in a direct exchange for more upper stage inert mass. At the 90%, 80% point, the payload is 18 kg. Reducing it to 16 kg would double the 2-kg stage hardware budget. This additional trade, to avoid difficulties in implementing tiny upper stages, can be considered at any point represented by Figs. 8 and 9.

For comparison with all of the two-stage possibilities, Table 5 shows the full range of single-stage options, including the region where two stages is theoretically preferred. The single-stage payload data place a limit on how much payload could be sacrificed in exchange with an upper stage. Note that a 90% stage can lift 17.2 kg by itself. If this propellant mass fraction could be achieved, then it would not be worth the trouble to develop an upper stage. The possibility of a single-stage MAV should be seriously considered, if one large liquid stage in the 80-kg range can be built with at least an 85% propellant fraction.

A major advantage of the single-stage option is that only one set of rocket hardware (tanks, engines, etc.) would need to be developed. For the same reason, it is worth asking what can be achieved by

Table 5 Mass breakdown of a single-stage liquid MAV having 74.5-kg propellant

Stage propellant fraction, %	Total stage mass, kg	Inert stage mass, kg	Payload mass, kg
74.5	100	25.5	0.0
80	93.2	18.6	6.8
83	89.8	15.3	10.2
85	87.7	13.2	12.3
88	84.7	10.2	15.3
90	82.8	8.3	17.2
95	78.5	3.9	21.5
100	74.5	0	25.5

Table 6 Stack of two identical liquid stages

Stage propellant fraction, %	Propellant mass, kg	Total stage mass, kg	Inert stage mass, kg	Payload mass, kg
63	31.47	49.95	18.5	0.1
65	31.90	49.1	17.2	1.9
70	32.90	47.0	14.1	6.0
75	33.81	45.1	11.3	9.9
80	34.63	43.3	8.7	13.4
85	35.38	41.6	6.2	16.7
90	36.07	40.1	4.0	19.8
95	36.70	38.6	1.9	22.7
100	37.27	37.3	0	25.5

stacking two identical stages. In Table 6, for each selected propellant fraction in the first column the propellant mass was adjusted to obtain the total required Δv. The total stage mass varies from half the gross launch mass at zero payload to half the single-stage propellant load when the stage hardware reaches zero.

The payload of identical stacked stages can be compared directly with that of a single stage in Table 5. For equal stage propellant fractions, there is just a slight improvement at the high end above 90%. At 85% and lower, the notion of two stacked stages appears to have more to offer. However, it is not easy to achieve the same propellant fraction at half-scale. Unlike the situation for a small upper stage, a smaller first stage would still have to deliver enough thrust for launch and efficient ascent. Even the best two-stage liquid MAV design cannot have a stage 1 propellant fraction as high as a single-stage MAV, for the same reason, that is, the stage 1 engine mass is essentially fixed. There is also the mass of separation hardware to contend with for any multistage option.

For an interesting perspective relative to conventional solids, a specific comparison for a single-stage MAV can be made with reference to Fig. 7 and Table 5. A 100-kg solid rocket MAV can launch a payload just over 12 kg if both stages are 85% (or 90 and 75% in combination). The upper-stage burnout mass is just 2.3 kg (or 3.3 kg). At the same 85% minimum propellant fraction, a single 88-kg liquid stage offers the same 12-kg payload, without the need to miniaturize technology further for an upper stage.

Mars Ascent Vehicle Shape

Returning now to the list of propulsion trade questions for Mars ascent, the second question is motivated by the constraints of Earth-to-Mars transportation. The shape of aeroshells needed to decelerate upon arrival in Mars's atmosphere, as well as stability after landing, requires the landed package to be wide and short. A long, narrow MAV would most likely land on Mars in a horizontal orientation. It would need a tilt-up mechanism for a vertical launch or a way to set the azimuth for a nonvertical launch. The ideal MAV would perhaps avoid both by fitting on a Mars lander while oriented for a vertical launch.

Considerations of packaging, structural load paths, and balancing all lead to a relatively tall, narrow stack for a two-stage solid rocket, based on conventional technology. Even if a short, stout solid-propelled MAV could be built, its atmospheric drag would be prohibitively high at conventional thrust levels. The delivered Δv requirement would increase to overcome higher drag, while following a less efficient steeper trajectory closer to path B.

Table 7 Importance of liquid MAV frontal area

Parameter	Table 4 liquid MAV	High drag liquid MAV
Frontal area	0.2 m^2	0.5 m^2
Total Δv to orbit	4157 m/s	4283 m/s
Launch Δv	3900 m/s	3889 m/s
Δv to circularize	257 m/s	394 m/s
Apoapsis longitude	78.9 deg	59.4 deg
Peak drag	69 N	148 N
Integrated drag	6580 N-s	12,150 N-s
Launch propellant	72.3 kg	72.2 kg
Total propellant (single-stage equiv.)	74.5 kg	75.6 kg

The answer is not quite as clear for the shape of a lower-thrust MAV. Liquid stage designs having side-by-side tanks have been proposed in the past, for example, four tanks to balance unequal masses of two liquids. Mars ascent simulations for a 100-kg liquid MAV were run with a higher, 0.5-m^2 frontal area. Other parameters remained unchanged from the baseline case. The trajectory results are compared in Table 7. As would be expected, the trajectory is slightly closer to path B than the baseline liquid trajectory indicated in Table 4 and in Fig. 4.

The less efficient high-drag liquid trajectory is still better than the baseline solid rocket trajectory. For single-stage vehicles, a short and wide 100-kg liquid MAV needs to have 1.1 kg less hardware and 1.1 kg of additional propellants, if other mission elements are unaffected.

Alternatively, the change implies a 4.5% overall mass growth for the MAV, if its empty mass is held constant and extra propellant is added to obtain the higher Δv. The implication is that a short, wide MAV works if $\geq$5 kg can be saved from the lander, such as by avoiding a tilt-up launch mechanism.

However, note that the drag coefficient was not changed, only the frontal area. A short MAV would most likely have a higher drag coefficient, even with aerodynamic shrouding heavier than the nose cone of a tall MAV. In addition to quantifying these changes individually, their net effect would have to be considered in view of design information for a tilt-up launch mechanism. What is certain is that Mars ascent drag is significant enough to strongly influence design decisions for any 100-kg MAV, regardless of the propellant choice.

Solid Thrust Reduction

The third through fifth questions in the list of propulsion trade questions for Mars ascent ask what can be gained by adjusting thrust magnitude, to reach the best compromise between drag losses and gravity losses. The best launch thrust at $I_{SP} = 280$ s was found to be in the range 1000–2000 N. It is not a sharp optimum.

Typically for solid propulsion applications, the propellant quantity and thrust are not independently selected. Burn rates are largely determined by propellant formulation, exposed area, and chamber pressure. Propellant additives that slow the reaction can affect specific impulse. Reducing the exposed area can impose packaging and structural constraints, for example, a narrower end-burning grain would increase vehicle length by the same factor as its thrust reduction. Pressure changes affect the burn rate only weakly. A larger nozzle would be required, for example, for half thrust at one-fifth pressure.[16] Nevertheless, it is worth considering that a combination of changes could halve the thrust. If such changes were to reduce the propellant fraction and I_{SP}, the relevant question then is whether improved trajectory performance could more than compensate for reduced rocket vehicle performance.

To explore the reduced-thrust option, ascent simulations were performed at 5000 N, half the nominal thrust. All other aspects of the conceptual solid-propelled MAV remained the same as in the baseline case. Table 8 shows that the required Δv falls by about 100 m/s. The half-thrust trajectory has a much lower drag peak, before motor burnout. The minor change in integrated drag indicates greater duration, which results from lower altitudes initially, closer to path A.

Table 8 Effect of halving solid MAV thrust

Parameter	Table 4 Solid MAV	Half-thrust solid MAV
Launch thrust	10,000 N	5,000 N
Total Δv to orbit	4371 m/s	4272 m/s
Launch Δv	2803 m/s	2985 m/s
Δv to circularize	1567 m/s	1287 m/s
Apoapsis longitude	19.6 deg	24.3 deg
Peak drag	852 N	394 N
Integrated drag	11,850 N-s	10,940 N-s
Launch propellant	64.0 kg	66.3 kg
Total propellant (single-stage equiv.)	79.7 kg	78.9 kg

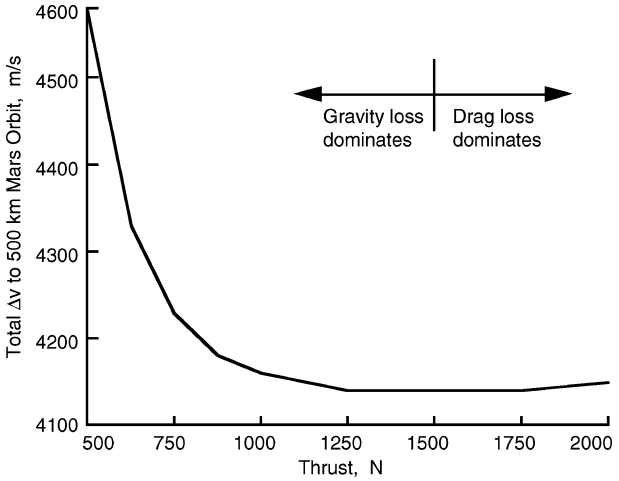

Fig. 10 Effect of thrust at $I_{SP} = 310$ s.

The apogee conditions are consistent with the path change, that is, the greater longitude and reduced Δv to circularize. A possible drawback is that the Δv split is further from even, compared to the baseline.

The ratio of the Δv totals in Table 8 is consistent with a reduction in I_{SP} from 280 to 274 s. Thus if the burn rate could be halved by using a propellant formulation that sacrificed less than 6 s of specific impulse, it might be worth examining. Alternatively, the last row in Table 8 shows that almost an extra kilogram of stage hardware would be allowable for design changes that can reduce thrust by 50%. Obtaining the exact numbers requires a staging analysis because reducing thrust is only of interest for stage 1.

Liquid Thrust Selection

Liquid propulsion is free from underlying constraints on thrust level. To avoid excess engine mass and to improve packaging, extra thrust is usually avoided. Mars launch simulations were repeated to find the minimum required Δv as a function of thrust (Fig. 10). The gravity loss increases steeply at the left side of the graph because thrust equals Mars liftoff weight at 375 N.

If engine mass did not matter, the ideal thrust would be in the range 1250–1500 N. In reality, a better choice is further to the left. There is no mission advantage to increasing thrust toward 2000 N because engine mass and the required Δv would both increase. In this context, the practical definition of engine mass is all stage hardware that can be made lighter if thrust is reduced. The derivative of mass with respect to thrust can be used, in combination with Fig. 10, to find a preferred design point.

The Earth weight of large launch vehicle engines is about 1% of thrust, but small engines are relatively heavier. Table 9 was generated using the assumption that engine weight (on Earth) is about 2% of thrust. More precisely, the derivative of inert mass with respect to thrust is 0.002 kg/N. Required Δv is from Fig. 10. In Table 9, burnout mass and available Δv vary, from the 1000-N baseline case, under the assumption that hardware mass trades directly with propellant in a single-stage 100-kg MAV. The point of departure uses the preceding data for a single-stage 100-kg MAV at 1000-N thrust.

Table 9 Net effect of engine mass

Thrust, N	Required Δv, m/s	Burnout mass, kg	Available Δv, m/s	Excess Δv, m/s
500	4602	24.453	4279	−323
625	4326	24.703	4248	−78
750	4225	24.953	4217	−8
875	4178	25.203	4187	+9
1000	4157	25.453	4157	0
1250	4140	25.953	4098	−42
1500	4141	26.453	4040	−101
2000	4152	27.453	3927	−255

The last column in Table 9 shows that a small reduction in thrust, to 875 N, improves the baseline case. There would be a greater incentive to reduce thrust if heavier engine technology is used, but the curve in Fig. 10 quickly becomes a wall below 750 N. A practical point worth noting is that custom lightweight hardware is needed. Although thrust and mass are not easily varied after implementation begins, the total mass of a liquid MAV might grow, over the course of its development program. For this reason, it might be better to err toward higher thrust. When the thrust trade results are viewed in this light, the 1000-N thrust magnitude appears to be a good starting point for a 100-kg MAV design.

Another question raised in the list of propulsion trade questions for Mars ascent for liquid propulsion is whether it makes sense to consider a sustainer burn to keep the tanks settled. In the baseline trajectory of Fig. 4, the ascent burn ends at 220 s, and the apoapsis is reached at 1730 s after launch. A 1-N thrust magnitude for example can be sufficient for settling. Over the 1510-s time period, propellant consumption would be 0.5 kg at $I_{SP} = 310$ s and at most 1 kg if the settling thrusters have a much lower specific impulse. Less Δv would be needed to circularize. If the hardware mass for microgravity propellant acquisition approaches 1 kg, then it would make sense to consider a continuous settling burn.

Three-Stage Solid MAV

Considering that the trajectory results do not favor a solid-propelled MAV, it is worth asking what else can be done to reduce drag. A concept based on Ref. 7 seeks to minimize drag, by using a three-stage trajectory. First, there is a vertical launch to a point just above most of the atmosphere. Then there are two more burns, which can nearly use path A from the higher starting point. The vertical launch reduces drag in two ways. It uses the shortest path through the atmosphere. Also, average speed through the atmosphere is reduced because the vehicle coasts to altitude after a minimum burn.

If the initial altitude reached by stage 1 is too high, the trajectory will be inefficient like path B. Analytical calculations show that above 54 km the ideal three-stage Δv exceeds 4371 m/s, that is, even in vacuum it cannot improve upon the two-stage atmospheric case in Table 4. If the initial altitude goal is too low, then the first stage becomes moot, and the three-stage MAV merely follows the two-stage trajectory.

The three-stage ascent scenario was simulated for a 100-kg MAV. Results indicate that the least total Δv occurs when the first stage lofts the vehicle to 25 km above Mars. The maximum drag is only 15% of the Fig. 5 peak. However, the advantage over the two-stage case is a slight 12 m/s, at 4359 m/s total to orbit. It is not a sharp optimum, as results are all in the range 4371 ± 20 m/s for altitudes between 0 and 40 km.

In general, there is the potential for a three-stage vehicle to lift a greater payload than two stages. However, the Δv split required by the specialized three-stage trajectory is far from ideal. The middle stage must deliver more velocity than the main stage of a two-stage solid MAV. Only about 500 m/s each is needed from the first and third stages, depending on initial altitude. Considering the small apoapsis burn, the first two stages constitute a MAV that has an "upside-down" Δv split. In summary, the three-stage MAV offers virtually no Δv reduction, and the stage miniaturization problem becomes more difficult.

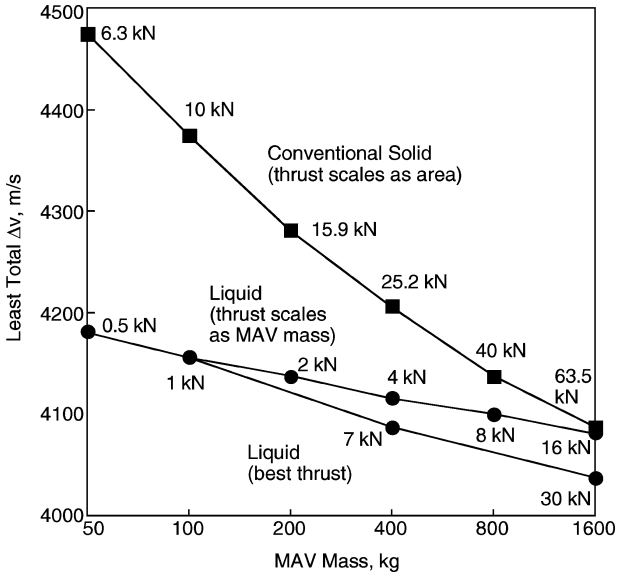

Fig. 11 Effect of MAV mass on required Δv.

Larger and Smaller MAV Sizes

Figure 11 shows how the trajectory results change when the MAV mass is varied. The drag area was scaled as the $\frac{2}{3}$ power of mass. Liquid thrust was scaled as mass, while solid thrust was scaled in proportion to area, consistent with a constant burn rate over an exposed area. Neither scaling rule for thrust is ideal, and so a third curve shows the best results obtained.

The solid thrust-to-mass ratio falls as the vehicle is scaled up, so that the drawbacks of high thrust are diminished. Although the scaling rules for the solid and nominal liquid would result in equal thrust at 100 tons, the curves also cross near 1.6 tons because the linearly scaled liquid thrust is not ideal. It is clear that the relatively high thrust typical of conventional solid rockets is a desirable characteristic on a large scale, but becomes detrimental as a MAV is scaled down.

Conclusions

The main result from the trajectory simulations is that Mars atmospheric drag is significant to ascent vehicles, if sized for affordable sample return. The high thrust of conventional solid rocket motors tends to increase drag, which requires a steeper, less efficient path to orbit. Reducing thrust, for less drag, is a worthy goal for solid rocket technology development directed toward a smaller MAV. The trajectory effects that tend to disfavor conventional solids become less pronounced as a MAV is scaled up.

Additional realism in the trajectory simulations would be unlikely to change the conclusions. For instance, the velocity of planet rotation (240 m/s at the equator, neglected herein) is aligned with path A. Planet rotation thus favors trajectories closer to path A than to path B, for eastward launches. Deliberate steering would not improve the conventional solid trajectory more than the liquid one because short burn times diminish the potential for path modification by guidance.

Staging calculations based on trajectory simulations show that a liquid-propelled MAV could carry more payload mass than a MAV based on conventional solid rocket motors, if the two propulsion technologies offered the same stage propellant fractions. For either solid or liquid, the necessarily high mass fractions have never been achieved on the scale of interest. Small conventional solid motors are more than 85% propellant, but it is a challenge to provide thrust vector control with very little extra mass. Flexible on/off control might also be of value to permit the staging point to be selected independently from trajectory events. Although liquid rocket technology offers ease of control at preferred thrust levels, a major challenge is to reduce hardware mass to far below that of conventional pressure-fed satellite propulsion, for example, by scaling down pump-fed launch vehicle technology.

An upper stage for any 100-kg MAV would need extreme miniaturization down to the order of 10 kg, with relatively little tolerance for sacrificing propellant fraction. Technology development efforts toward high propellant fractions are more likely to succeed on a scale closer to 100 kg than to 10 kg. If stage propellant fractions can approach 90% along with a flexible thrust profile, a single-stage Mars ascent vehicle would be a viable alternative to further miniaturization.

Acknowledgment

This work was performed under the auspices of the U.S. Department of Energy by the University of California, Lawrence Livermore National Laboratory, under Contract W-7405-Eng-48.

References

[1]Space Studies Board, NRC, *New Frontiers in the Solar System: An Integrated Exploration Strategy*, National Academy Press, Washington, DC, 2003.

[2]Kerr, R. A., "Rainbow of Martian Minerals Paints Picture of Degradation," *Science*, Vol. 305, No. 5685, 2004, pp. 770, 771.

[3]Weaver, W. L., "Mars Surface-to-Orbit Vehicles for Sample Return Missions," *Journal of Spacecraft and Rockets*, Vol. 11, No. 6, 1974, pp. 426, 427.

[4]Wercinski, P. F., "Mars Sample Return: A Direct and Minimum-Risk Design," *Journal of Spacecraft and Rockets*, Vol. 33, No. 3, 1996, pp. 381–385.

[5]Guernsey, C. S., "Mars Ascent Propulsion System (MAPS) Technology Program: Plans and Progress," AIAA Paper 98-3664, July 1998.

[6]Reichhardt, T., "The One-Pound Problem," *Air and Space Smithsonian*, Vol. 14, No. 4, 1999, pp. 50–57.

[7]Wilcox, B. H., "Miniature Ascent Vehicles Derived from the Navy's Air-Launched Satellite Developed in 1958," AIAA Paper 2001-3879, July 2001.

[8]Stephenson, D., "Mars Ascent Vehicle—Concept Development," AIAA Paper 2002-4318, July 2002.

[9]Baker, A. M., and Coxhill, I., "Chemical Propulsion Systems for Low Cost Mars Sample Return," AIAA Paper 2004-3492, July 2004.

[10]Whitehead, J. C., "Mars Ascent Propulsion Options for Small Sample Return Vehicles," AIAA Paper 97-2950, July 1997.

[11]Whitehead, J. C., and Guernsey, C. S., "Mars Ascent Propulsion on a Minimum Scale," *Acta Astronautica*, Vol. 45, Nos. 4–9, 1999, pp. 319–327.

[12]Whitehead, J. C., and Brewster, G. T., "High Pressure Pumped Hydrazine for Mars Sample Return," *Journal of Spacecraft and Rockets*, Vol. 37, No. 4, 2000, pp. 532–538.

[13]Desai, P. N., Braun, R. D., Engelund, W. D., Cheatwood, F. M., and Kangas, J. A., "Mars Ascent Vehicle Flight Analysis," AIAA Paper 98-2850, June 1998.

[14]Helgostam, L. F., "Requirements for Efficient Mars Launch Trajectories," *Journal of Spacecraft and Rockets*, Vol. 1, No. 5, 1964, pp. 539–544.

[15]Seiff, A., and Kirk, D., "Structure of the Atmosphere of Mars in Summer at Mid-Latitudes," *Journal of Geophysical Research*, Vol. 82, No. 28, 1977, pp. 4364–4378.

[16]Sutton, G. P., *Rocket Propulsion Elements, An Introduction to the Engineering of Rockets*, 6th ed., Wiley, New York, 1992, pp. 374, 375.

C. Kluever
Associate Editor